SYNTHESIS, CHARACTERIZATION AND EVALUATION OF CO-OXIDATION CATALYSTS FOR HIGH REPETITION RATE CO_2 TEA LASERS

Thomas P. Moser
Hughes Aircraft Company
Electro-Optical and Data Systems Group
El Segundo, California

ABSTRACT

An extremely active class of noble metal catalysts supported on titania was developed and fabricated at Hughes for the recombination of oxygen (O_2) and carbon monoxide (CO) in closed-cycle CO_2 TEA lasers. The incipient wetness technique was used to impregnate titania and alumina pellets with precious metals including platinum and palladium. In particular, the addition of cerium (used as an "oxygen storage" promoter) produced an extremely active $Pt/Ce/TiO_2$ catalyst. By comparison, the complementary $Pt/Ce/\gamma\text{-}Al_2O_3$ catalyst was considerably less active. In general, chloride-free catalyst precursors proved critical in obtaining an active catalyst while also providing uniform metal distributions throughout the support structure. Detailed characterization of the $Pt/Ce/TiO_2$ catalyst by both SEM and EDX analyses demonstrated uniform dendritic crystal growth of the metals throughout the support, while ESCA analysis was used to characterized the oxidation states of Pt, Ce and Ti. The performance of the catalysts was evaluated with an integral flow reactor system incorporating real time analysis of O_2 and CO. With this system, the transient and steady-state behavior of the catalysts were evaluated. The kinetic evaluation was complemented by tests in a compact, closed-cycle Hughes CO_2 TEA laser operating at a pulse repetition rate of 100 Hz with a catalyst temperature of 75 to 95°C. The $Pt/Ce/TiO_2$ catalyst was compatible with a $^{13}C^{16}O_2$ gas fill.

INTRODUCTION

Long lifetime, high repetition rate CO_2 TEA lasers are required for a number of important applications including advanced rangefinding and chemical detection. The primary life-limiting process of such lasers is the generation of oxygen or some unknown coincidentally formed species in the glow discharge. If such a

species accumulates to a sufficient concentration, the discharge can rapidly degenerate into an arcing process. To prevent arcing, a catalyst can be used to maintain oxygen levels and other deleterious species below consequential levels.

With the increasing demand for high energy, rapidly pulsed CO_2 lasers, considerable attention has been given to the application of CO oxidation catalysts in sealed lasers (1-16). For the most part, however, these investigations have been concerned with the testing of commercial CO oxidation catalysts not necessarily designed for laser applications.

The first extended operation of a sealed TEA laser was reported by Stark et al (1). Operating with high CO_2 levels (eg. 60% CO_2, 40% N_2, 0% He), they demonstrated the continuous operation of a 1 Hz laser aided by a hot (1100^oC) platinum wire catalyst. Quantitative details regarding the performance of the platinum wire catalyst were provided by Stark and Harris (2). The hot wire approach was significantly limited in application, however. For high repetition rate devices, both rapid recirculation and cooling of the internal gases are required. Correspondingly, increased catalytic activity would be required to compensate for the increased oxygen production. Under such conditions, a hot platinum wire would consume a prohibitive amount of energy, while introducing an enormous heat removal problem.

With ever stringent engineering constraints posed by laser designs, the practical catalytic solution will likely include a "low temperature" (20 to 100^oC) CO oxidation catalyst, preferably in either a monolithic or pellet form. Although highly active at low temperature, Hopcalite (60% MnO_2, 40% CuO) has demonstrated only limited success (3), primarily because of its propensity to form dust and to deactivate by CO_2 adsorption and water contamination. Other catalytic systems include both alumina (Al_2O_3) (4, 5) and tin oxide (SnO_2) (6-15) supported precious metals. In particular, the catalysts which utilize an SnO_2 support have received much attention, primarily because of their reported low temperature capabilities and compatibility with isotopic $^{12}C^{18}O_2$ lasers.

The present investigation involves the fabrication, characterization and evaluation of a new class of precious-metal laser catalysts supported on titania (TiO_2) which use cerium as an "oxygen storage promoter" for improved low temperature activity. As an example, the detailed synthesis, characterization and evaluation of a robust (pellet) $Pt/Ce/TiO_2$ catalyst are presented. Results with a TEA laser using both $^{12}C^{16}O_2$ and $^{13}C^{16}O_2$ are also summarized.

EXPERIMENTAL

Support Material

Titania

The titania support was supplied as 1/8 inch extrudates from Norton Company as a 90/10 mixture of the anatase and rutile phases, respectively. Surface area analysis by the BET method yielded 34 m^2/gram with an average pore diameter of 73 angstroms.

Alumina

The alumina support was supplied as 3.2 mm diameter spheres (Grace LBD) consisting primarily of gamma phase alumina. The BET surface area was 110 m^2/gram.

Catalyst Preparation

The incipient wetness technique was used to impregnate blank titania (TiO_2) and alumina (γ-Al_2O_3) pellets with platinum, palladium, and cerium. Chloride-free catalyst precursors including tetraammineplatinum (II) nitrate, $[Pt(NH_3)_4](NO_3)_2$, tetraammine-palladium (II) nitrate, $[Pd(NH_3)_4](NO_3)_2$, and cerium nitrate, $Ce(NO_3)_3 \cdot 6H_2O$ were used as the source of platinum, palladium, and cerium, respectively. The specific pore volume of the support material was determined by measuring the saturation volume (pore volume as measured for a specific solvent) volumetrically with water. Once this saturation volume was known, a volumetric solution composed of the appropriate metal salts was prepared with a prescribed concentration level. This quantitative solution was then mixed with the appropriate mass of blank support, resulting in the physical adsorption of the solution onto the surface and into the interior of the pellet. A slight excess (ca. 5%) of solution was used in the impregnation procedure to allow uniform and complete saturation. The residual solution was retained for recovery and analysis. The catalyst preparation was completed by slowly drying the "wetted" catalyst pellets in a flowing air hood followed by activation in flowing helium (200°C; 2h), calcination in flowing oxygen (400°C; 4h), and reduction in flowing hydrogen (300°C; 4h). The metal loadings were determined by a material balance, taking into account the concentration of metal in the solution and the saturation volume of the support material.

Catalyst Characterization

BET Surface Area

A Quantasorb Jr. (Quantachrome Corporation) was used to measure surface areas by employing the single point BET method with nitrogen as the adsorbate.

Scanning Electron Microscopy (SEM)

Scanning electron micrographs were obtained with a Cambridge Stereoscan 250 Mk 3 Scanning Electron Microscope equipped with an EDAX PV9100 Energy Dispersive X-ray (EDX) analysis system. Micrographs were obtained with a backscattering detector, while a windowless detector was employed for EDX elemental detection down to the atomic weight of carbon.

Electron Spectroscopy for Chemical Analysis (ESCA)

Information concerning the oxidation states of Pt, Ce, and Ti were obtained by ESCA analysis. A Perkin Elmer 5500 ESCA/SAM with MgK_{α} X-rays was used with a chamber pressure of approximately 10^{-9} torr. Spectra were referenced to the C 1s covalent peak at 284.6 eV.

Catalyst Evaluation

Figure 1 shows the flow scheme for the low flow catalyst test station. A certified gas mixture having a composition of 0.5% oxygen, 1.0% CO, 17% nitrogen, 17% CO_2 and the balance helium was used for routine catalyst evaluation. Other gases including hydrogen, carbon monoxide, oxygen and helium were also deliverable for special processes, such as catalyst conditioning. The combination of high precision rotameters (Fisher Porter Model 10A3555) and individually calibrated mass flow controllers (Tylan Model FC-280) allowed for accurate and reproducible gas flow rates and the synthesis of special gas blends. The system pressure was monitored by an absolute pressure transducer/indicator. For real time gas analysis, a specifically tuned Beckman Industrial nondispersive infrared analyzer (Model 868) was used for CO analysis, while a Beckman oxygen analyzer (Model 755A) monitored oxygen levels.

The reactor was fabricated from standard wall Pyrex tubing having an inner diameter of nominally 0.5 inches and a length of 15 inches (Figure 2). The catalyst pellets were charged to the reactor

together with Pyrex spheres (1/8 inch in diameter) which served to minimize radial temperature gradients. The catalyst zone was held in place by "plugs" of Pyrex wool. The catalyst bed temperature was monitored with a sub-miniature type K sheathed thermocouple. The reactor was oriented vertically.

The catalytic activity for both CO and oxygen disappearance was calculated as:

$$\text{Activity} = \frac{Q\ (X_i^{\text{inlet}} - X_i^{\text{outlet}})}{V_c} \qquad (1)$$

where Q = flow rate across catalyst bed (standard cm^3/min)
X_i = mole fraction ($i = O_2$, CO)
V_c = volume of catalyst bed including void volume (cm^3)

Laser Testbed

A sealed modular TE laser was used to investigate catalytic performance. The transmitter used a corona discharge for preionization with transverse gas flow. The modular approach was chosen to allow for both a compact 1 to 3 Hz source or as a 100 Hz device with the straightforward addition of a flow module. The fully integrated, closed-cycle modular laser assembly shown in Figure 3 consisted of, from top to bottom, a potted PFN, discharge module and optical bench, a side mounted catalyst/heat exchanger section, and a tangential fan. A more detailed description of the device was given previously (17).

RESULTS AND DISCUSSION

Role of Catalytic Precursors

The selection of an appropriate chemical complex type for Pt, Pd and Ce proved extremely critical for synthesizing an active catalyst. In particular, catalyst samples prepared with chloride-free metal salts such as tetraammineplatinum (II) nitrate, tetraamminepalladium (II) nitrate and cerium nitrate resulted in deep penetration of the metals into the interior of the titania pellet. By contrast, catalysts prepared with chloride-based metals, including

hexachloroplatinic acid-6-hydrate, resulted in "eggshell" metal distributions in the support structure. In all cases, the chloride-free preparations resulted in superior catalytic performance. The relatively lower catalytic activity associated with the chloride-based preparations resulted from poor metal dispersion coupled with the inactive nature of metal sites complexed with chloride ions.

Catalyst Supports and Promoters

Figures 4 and 5 show respectively the O_2 and CO disappearance activity for a series of Pt, Pd, Pt/Ce, and Pd/Ce catalysts supported on titania. The 2.0 wt% Pt/2.0 wt% Ce ($Pt/Ce/TiO_2$) catalyst clearly demonstrated the highest activity throughout the 25 to 200°C temperature range. The analogous 2.0 wt% Pd/2.0 wt% Ce ($Pd/Ce/TiO_2$) catalyst was not only less active than the $Pt/Ce/TiO_2$ variety, but also less active than the 4.4 wt% Pd (Pd/TiO_2) catalyst and the 3.8 wt% Pt (Pt/TiO_2) catalyst. Furthermore, the $Pd/Ce/TiO_2$ catalyst was the least active of the series. These results suggest a distinct synergistic effect between Pt and Ce which was not apparent between Pd and Ce. Moreover, the simple impregnation of Ce onto TiO_2 yielded an inactive material.

Inasmuch as alumina is one of the most common support materials, it provided a basis for comparison with other supported catalyst systems, particularly for metals supported on titania as in the present study. Figures 6 and 7 make a direct comparison between the 2.0 wt% Pt/2.0 wt% Ce on titania ($Pt/Ce/TiO_2$) catalyst and the 2.0 wt% Pt/2.0 wt% Ce on gamma alumina ($Pt/Ce/Al_2O_3$) catalyst. Since the titania and alumina pellets had different particle densities, the activities were normalized on both a volume and mass basis (Figures 6 and 7, respectively). Despite having a much lower surface area (34 versus 110 m^2/gram), the $Pt/Ce/TiO_2$ catalyst was considerably more active than the $Pt/Ce/Al_2O_3$ variety. Whereas the $Pt/Ce/TiO_2$ catalyst demonstrated considerable activity between 25 to 100°C, the $Pt/Ce/Al_2O_3$ catalyst was inactive in the same temperature range.

As with automotive catalysts (18), the addition of cerium apparently helps to balance the relatively weak adsorption of oxygen with the strong adsorption of carbon monoxide. Furthermore, as suggested by the above results, this "oxygen storage" property appears to be directly linked to a chemical interaction between Pt, Ce, and TiO_2.

In-Laser Testing

The modular CO_2 TE laser was tested for extended periods at a 100 Hz repetition rate in a completely sealed condition using the Hughes $Pt/Ce/TiO_2$ catalyst. Typically, the laser was operated for several hours at a time, turned off overnight, and restarted the next day. The test results are as follows:

-100 Hz repetition rate
-80 mJ/pulse, no fall off over time
-1 MW peak power
-$5x10^6$ total shots
-75 to 95°C catalyst temperature
-Operation with $^{12}C^{16}O_2$ or $^{13}C^{16}O_2$

The $Pt/Ce/TiO_2$ catalyst is currently being tested in a higher energy (250 mJ) device at 200 Hz.

Characterization of Hughes $Pt/Ce/TiO_2$ Catalyst

Scanning Electron Microscopy (SEM)

Figure 8 shows both a longitudinal and a transverse view of a sectioned catalyst pellet using a conventional high power microscope. The longitudinal cross section clearly shows a random distribution of Pt and Ce within the pores of the pellet. In addition, the extent of titania reduction or perhaps the density variation throughout the pellet is indicated qualitatively by the dark "band" about the pellet.

Using a backscattering SEM image technique, a mapping of the Pt/Ce distribution was obtained. Figure 9a clearly shows the dendritic crystal growth of both Pt and Ce in the TiO_2 matrix. Figure 9b shows a close-up view of Figure 9a point A. EDX analysis of the exterior of the pellet (side surface point B, Figure 9a) indicated considerable amounts of Pt and Ce. By contrast, the dark portion of the catalyst pellet as viewed in Figure 8 was void of both Pt and Ce as indicated by the EDX spectrum.

Electron Spectroscopy for Chemical Analysis (ESCA)

Information concerning the oxidation states of Pt, Ce and Ti were obtained by ESCA analysis. This information lends insight into the redox (reduction/oxidation) mechanism functioning at the catalytic surface.

Figure 10 shows the Pt 4f ESCA spectrum for the $Pt/Ce/TiO_2$ catalyst, including both the raw data and fitted curves reflecting the different chemical states of platinum. The Pt $4f_{7/2}$ peak at 70.6 eV and the Pt $4f_{5/2}$ peak at 73.9 eV correspond to metallic platinum (19, 20). The curve fitting analysis indicated the presence of both PtO (oxidation state of Pt^{+2}) and PtO_2 (oxidation state of Pt^{+4}). Likewise, the Ce 3d ESCA spectrum (Figure 11) also indicated multiple oxidation states. The Ce 3d peaks at both 885.3 and 903.6 eV correspond to metallic cerium (21). The fitted Ce 3d peak at 881.2 eV is associated with Ce_2O_3 (oxidation state of Ce^{+3}), whereas the fitted peak at 899.5 eV is associated with CeO_2 (oxidation state of Ce^{+4}). Since it is generally assumed that lattice oxygen is responsible for the catalytic oxidation of carbon monoxide (22), the presence of multiple oxidation states for both Pt and Ce suggests these metals may participate in a redox mechanism.

The corresponding 2p ESCA spectrum for Ti is given in Figure 12. In contrast with the Pt and Ce spectra, the Ti spectrum indicated only a single oxidation state. The Ti $2p_{3/2}$ peak at 458.4 eV and the Ti $2p_{1/2}$ peak at 464.1 eV are associated with the Ti^{+4} oxidation state of TiO_2 (20, 23).

CONCLUSIONS

The development of laser catalysts at Hughes has led to significant improvements in the performance of long-life repetitively pulsed closed-cycle CO_2 TEA lasers. Laser demonstrations in excess of 10^6 continuous shots at 100 Hz were facilitated by a Hughes $Pt/Ce/TiO_2$ catalyst functioning between 75 to 95°C. In addition, the compatibility of this catalyst was confirmed with an isotopic $^{13}C^{16}O_2$ TEA laser.

ACRONYMS

BET	Brunauer, Emmett, and Teller
EDX	Energy dispersive X-ray
ESCA	Electron Spectroscopy for Chemical Analysis
PFN	Pulsed frequency network
SEM	Scanning electron microscopy
TE	Transversely excited
TEA	Transversely-excited atmospheric pressure configuration

ACKNOWLEDGMENTS

The author wishes to thank Dan Demeo and Jerry Meldrum of the Hughes Technology Support Division for catalyst characterization by ESCA and SEM, respectively. In-laser catalyst testing and TE laser development were performed by Wayde Affleck, Dr. David Cohn, Robert Eldridge, and Mike Hasselbeck of the Hughes Advanced Tactical Programs Division and Dr. Tom Watson of the Hughes Industrial Products Division. The catalyst development work was supported by a Hughes independent research and development program.

REFERENCES

1. D. S. Stark, P. H. Cross and M. R. Harris: A Sealed, UV-Preionisation CO_2 TEA Laser with High Peak Power Output. J. Phys. E: Sci. Instrum., **11**, 1978, pp. 311-315.

2. D. S. Stark and M. R. Harris: Platinum-Catalysed Recombination of CO and O_2 in Sealed CO_2 TEA Laser Gases. J. Phys. E: Sci. Instrum., **11**, 1978, pp. 316-319.

3. R. B. Gibson, A. Javan, K. Boyer: Sealed Multiatmosphere CO_2 TEA Laser: Seed-gas compatible System Using Unheated Oxide Catalyst. Appl. Phys. Lett., **32**(11), 1978, pp. 726, 727.

4. C. Willis and J.G. Purdon: Catalytic Control of the Gas Chemistry of Sealed TEA CO_2 Lasers. J. Appl. Phys., **50**(4), 1979, pp. 2539- 2543.

5. M. S. Sorem and G. Faulkner: Catalytic Converters for Closed-Cycle Operation of Isotopic CO_2 TEA Laser. Rev. Sci. Instrum., **52**(8), 1981, p. 1193.

6. G. C. Bond, L. R. Molloy, and M. J. Fuller: Oxidation of Carbon Monoxide over Palladium-Tin (IV) Oxide Catalysts: An Example of Spillover Catalysis. J. Chem. Soc. Chem. Comm., 1975, pp. 796-797.

7. D. S. Stark and M. R. Harris: Catalysed Recombination of CO and O_2 in Sealed CO_2 TEA Laser Gases at Temperatures Down to $-27^{o}C$. J. Phys. E: Sci. Instrum., **16**, 1983, pp. 492-496.

8. D. S. Stark, Z. Crocker, and G. J. Steward: A Sealed 100 Hz CO_2 TEA Laser using High CO_2 Concentrations and Ambient Temperature Catalysts. J. Phys. E: Sci. Instrum. **16**, 1983, pp. 158-161.

9. C. F. Sampson and N. J. Gudde: The Oxidation of Carbon Monoxide using a Tin Oxide Catalyst. Closed-Cycle, Frequency-Stable CO_2 Laser Technology, NASA CP-2456, 1987.

10. H. T. Price and S. R. Shaw: High Repetition Rate Sealed CO_2 TEA Lasers using Heterogeneous Catalysts. Closed-Cycle, Frequency-Stable CO_2 Laser Technology, NASA CP-2456, 1987.

11. D. R. Schryer, B. D. Sidney, I. M. Miller, R. V. Hess, G. M. Wood, C. E. Batten, L. G. Burney, R. F. Hoyt, P. A. Paulin, K. G. Brown, J. Schryer, and B. T. Upchurch: NASA-LaRC Research on Catalysts for Long-Life Closed-Cycle CO_2 Laser. Closed-Cycle, Frequency-Stable CO_2 Laser Technology, NASA CP-2456, 1987.

12. B. T. Upchurch, G. M. Wood, R. V. Hess, and R. F. Hoyt: Rare Isotope Studies involving Catalytic Oxidation of CO over Platinum-Tin Oxide. Closed-Cycle, Frequency-Stable CO_2 Laser Technology, NASA CP-2456, 1987.

13. C. E. Batten, I. M. Miller, P. A. Paulin: Studies of CO Oxidation on Pt/SnO_2 Catalyst in a Surrogate CO_2 Laser Facility. Closed-Cycle, Frequency-Stable CO_2 Laser Technology, NASA CP-2456, 1987.

14. K. G. Brown and J. Schryer: Characterization of Pt/SnO_2 Catalysts for CO Oxidation. Closed-Cycle, Frequency-Stable CO_2 Laser Technology, NASA CP-2456, 1987.

15. B. D. Sidney: Studies of Long-Life Pulsed CO_2 Laser with Pt/SnO_2 Catalyst. Closed-Cycle, Frequency-Stable CO_2 Laser Technology, NASA CP-2456, 1987.

16. P. G. Browne and A. L. S. Smith: Long-Lived CO_2 Lasers with Distributed Heterogeneous Catalysis. J. Phys D: Appl. Phys., **7**, 1974, pp. 2464-2470.

17. D. B. Cohn, M. P. Hasselbeck, W. H. Affleck, R. E. Eldridge, T. P. Moser, G. R. Sasaki, T. A. Watson, and P. J. Bailey: Compact High Repetition Rate CO_2 TEA Lasers. SPIE, **1042**, CO_2 Lasers and Applications, 1989, pp. 63-69.

18. S. E. Oh and C. C. Eickel: Effects of Cerium Addition on CO Oxidation Kinetics over Alumina-Supported Rhodium Catalysts. J. Catal., **112**, 1988, pp. 543-555.

19. T. Sheng, X. Guoxing, and W. Hongli: The Nature of the SMSI State of the Pt/TiO_2 System. J. Catal., **111**, 1988, pp. 136-145.

20. G. B. Hoflund, A. L. Grogan, and D. A. Asbury: An ISS, AES, and ESCA Study of the Oxidative Reductive Properties of Platinized Titania. J. Catal., **109**, 1988, pp. 226-231.

21. J. Z. Shyu, W. H. Weber, and H. S. Gandhi: Surface Characterization of Alumina-Supported Ceria. J. Phys. Chem., **92**, 1988, pp. 4964-4970.

22. P. Mars and D. W. van Krevelen: Oxidation carried out by means of Vanadium-Oxide Catalysts. Chem. Eng. Sci., **3**, Spec. Suppl., 1954, pp. 41-59.

23. M. K. Bahl, S. C. Tsai, and Y. W. Chung: Auger and Photoemission Investigations of the $Pt\text{-}SrTiO_3$ (100) Interface: Relaxation and Chemical Shift Effects. Phys. Rev. B., **21**(4), 1980, pp. 1344-1348.

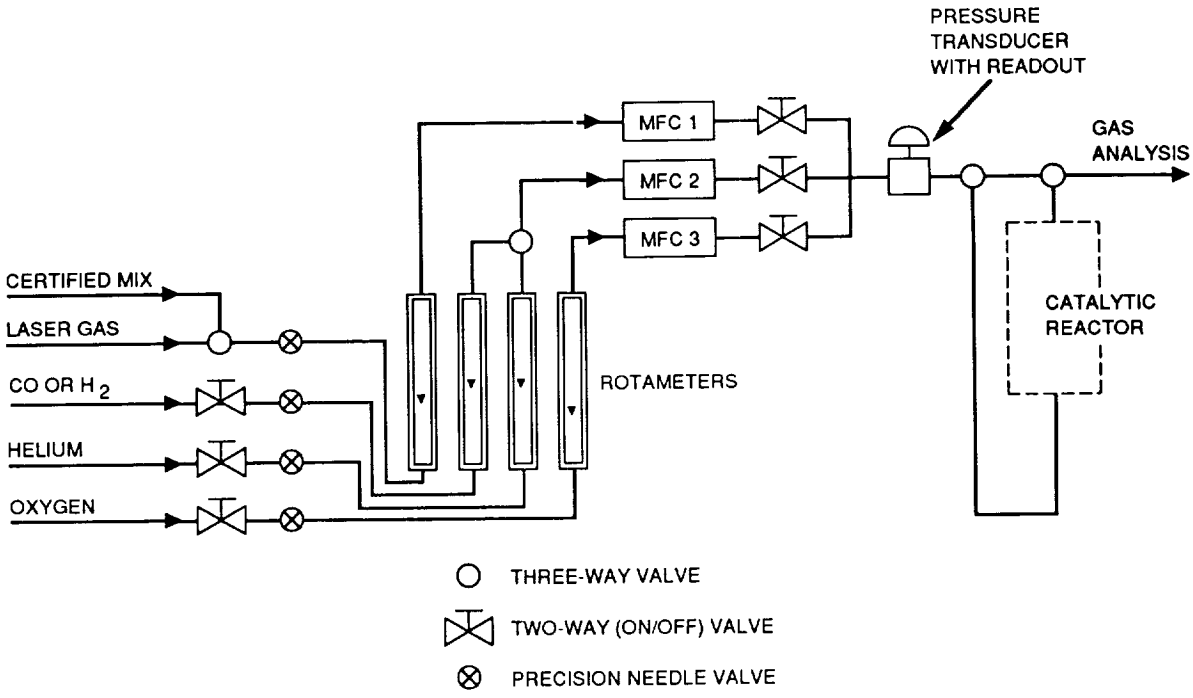

Figure 1. Flow scheme for low flow catalyst test station.

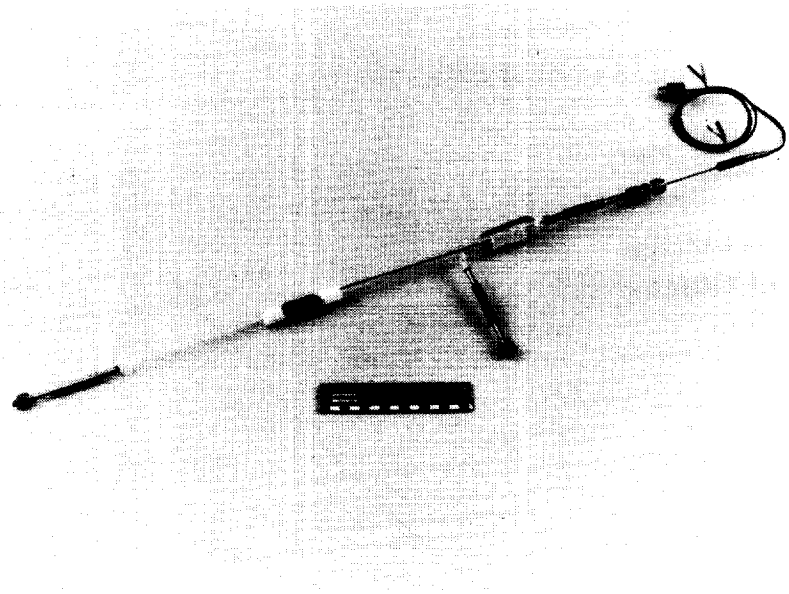

Figure 2. Catalytic reactor.

ORIGINAL PAGE
BLACK AND WHITE PHOTOGRAPH

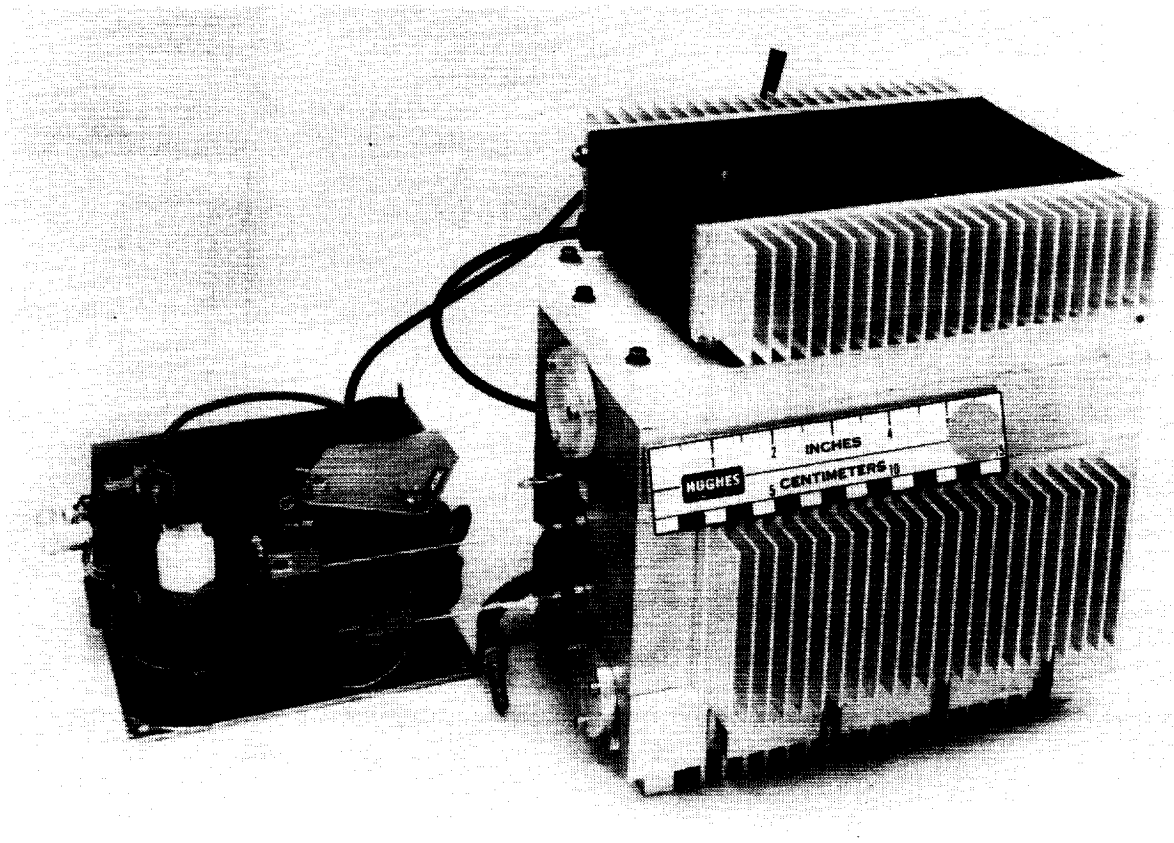

Figure 3. Modular TE laser.

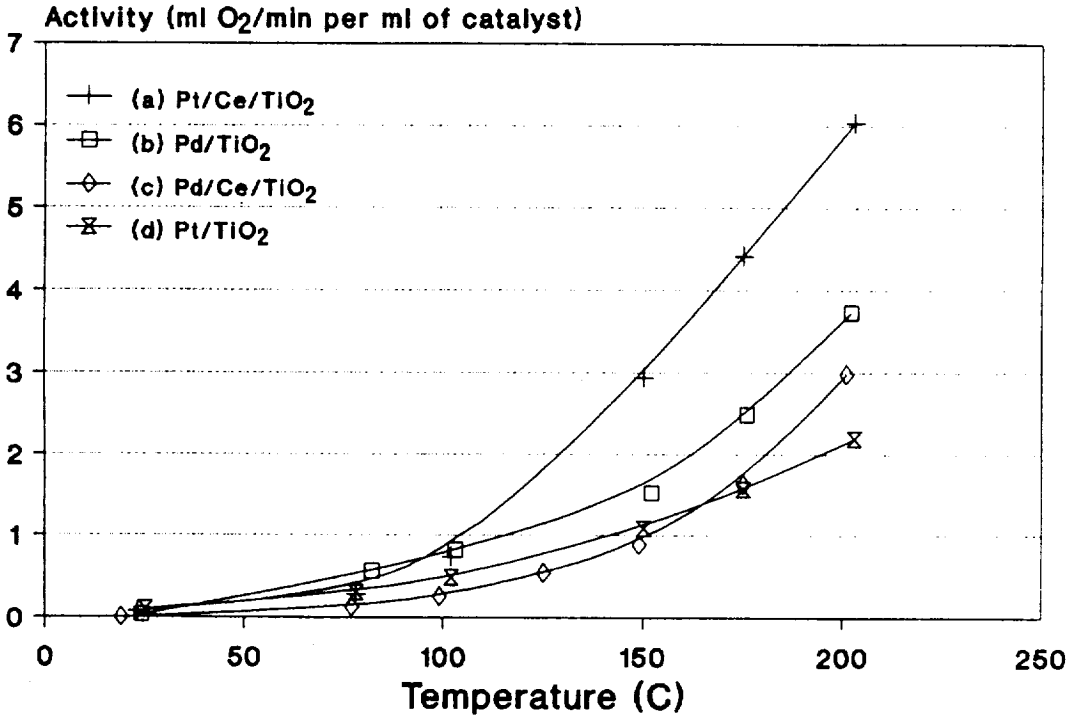

Figure 4. Oxygen disappearance activity for titania-supported Hughes catalysts.

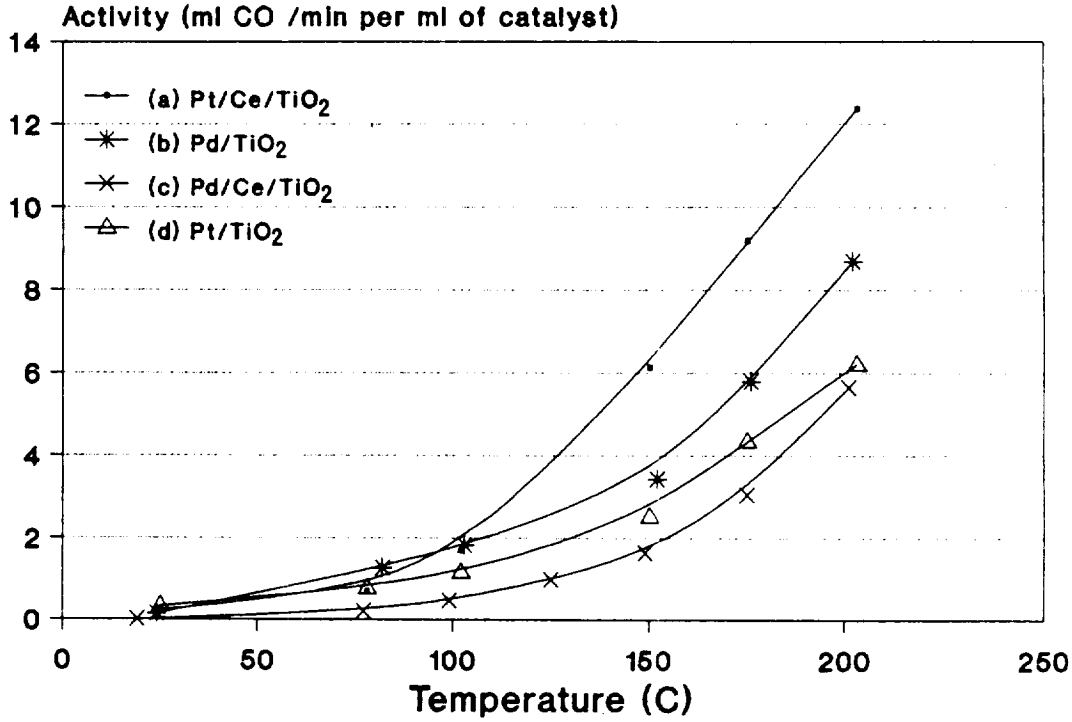

Figure 5. Carbon monoxide disappearance activity for titania supported Hughes catalysts.

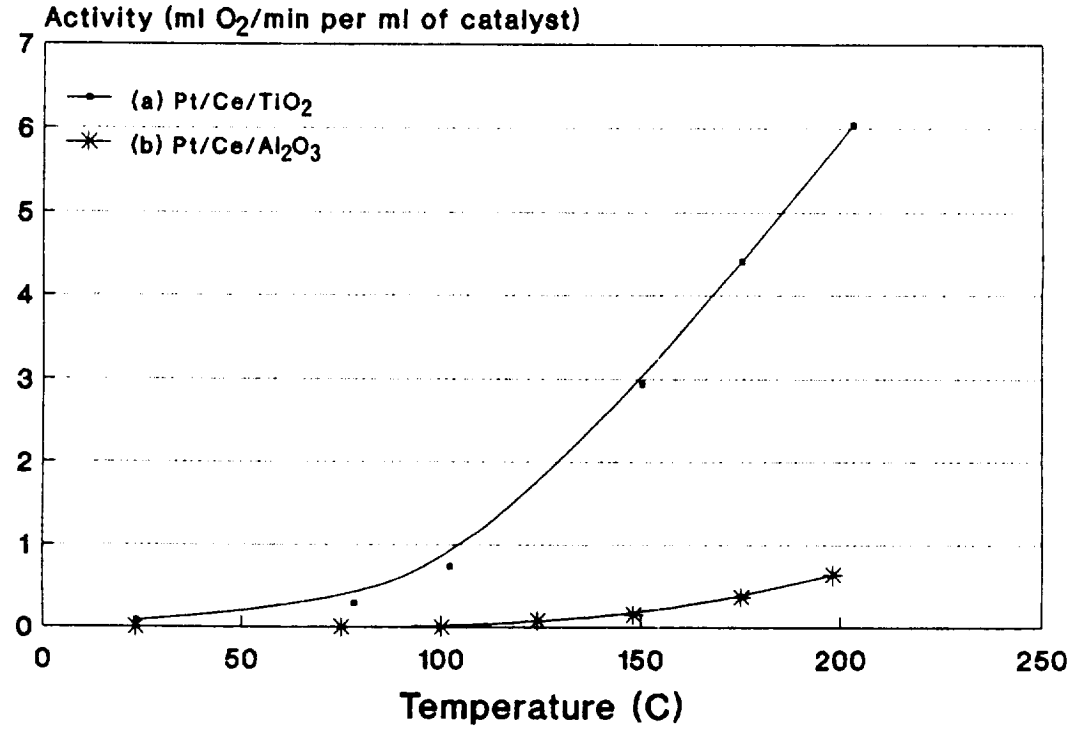

Figure 6. Comparison of alumina- and titania-supported Hughes Pt/Ce catalysts: Activity normalized on a volume basis.

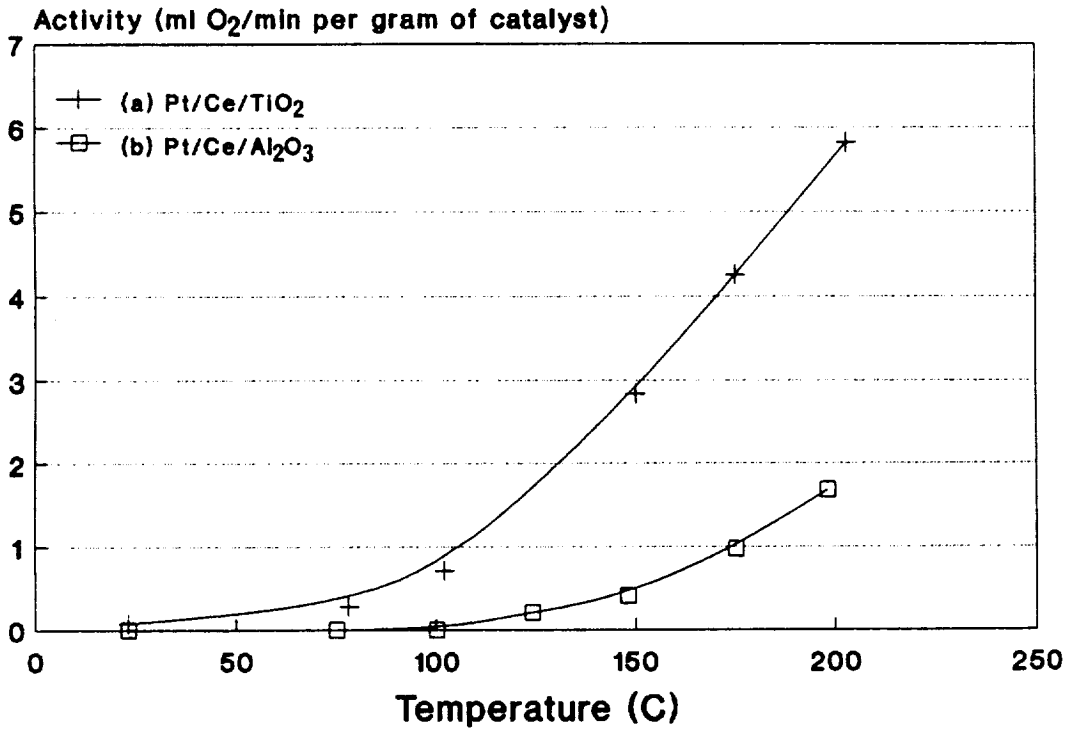

Figure 7. Comparison of alumina- and titania-supported Hughes Pt/Ce catalysts: Activity normalized on a mass basis.

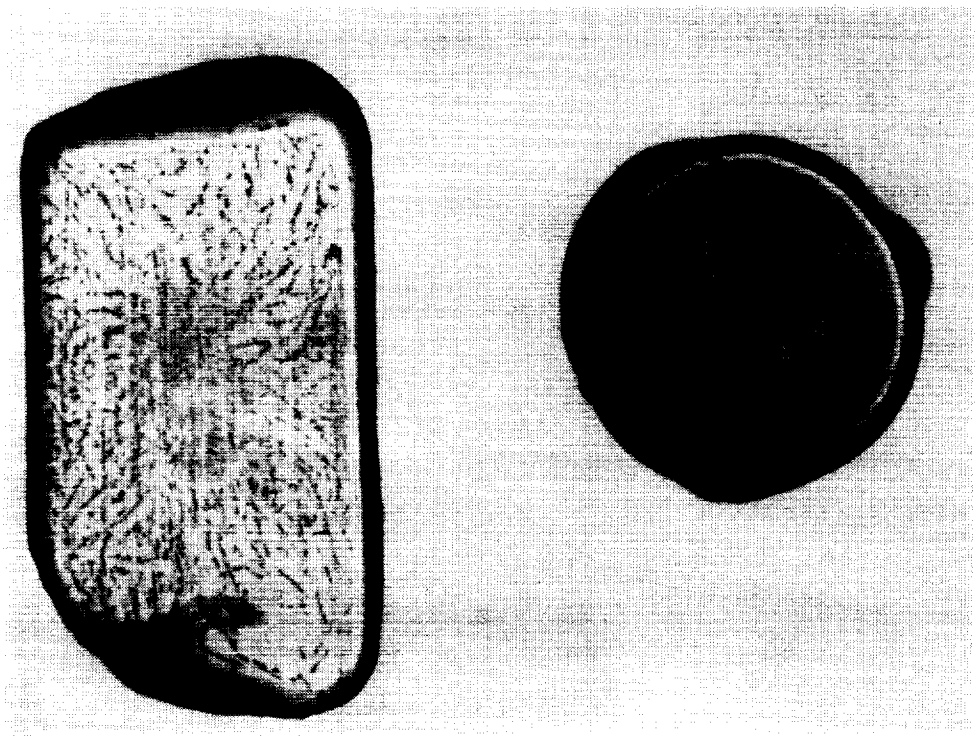

Figure 8. Longitudinal and transverse views of a sectioned Hughes Pt/Ce/TiO_2 catalyst pellet.

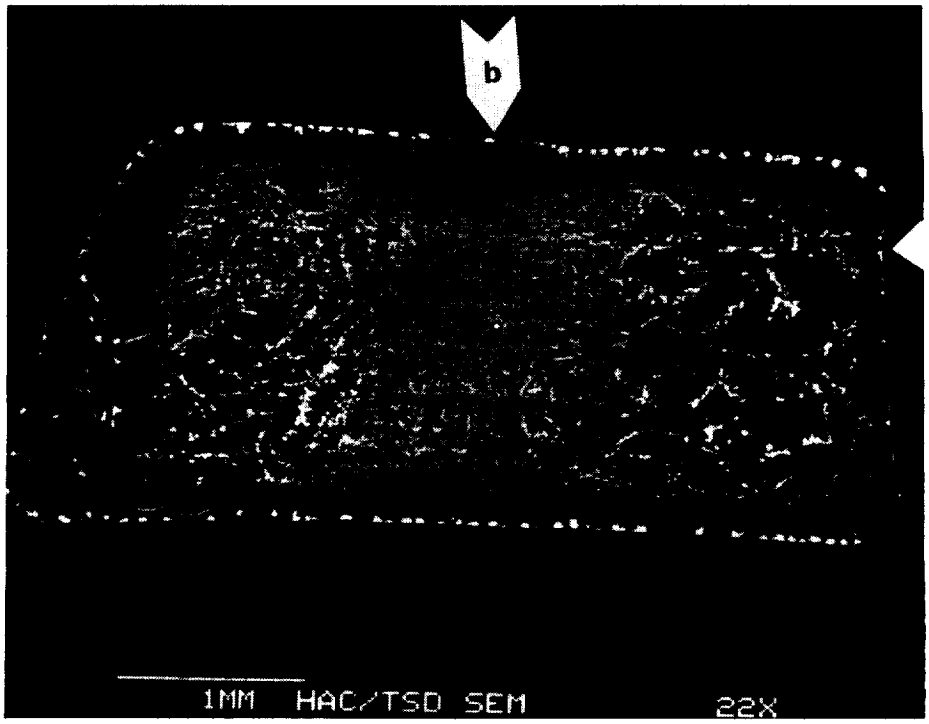

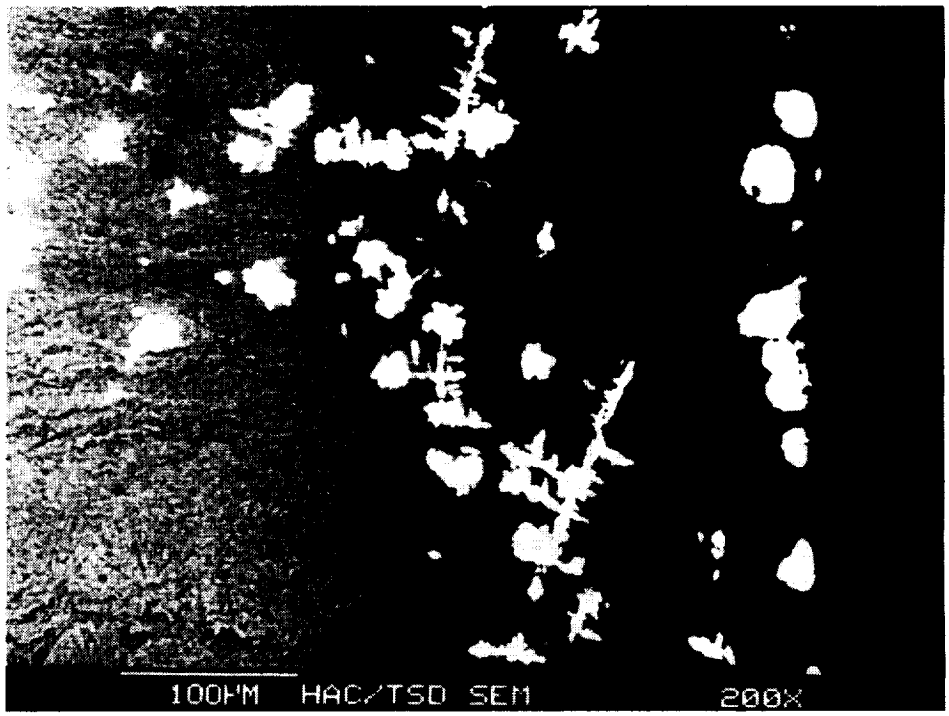

Figure 9. SEM backscattering image of a Hughes $Pt/Ce/TiO_2$ catalyst: (a) longitudinal view, (b) longitudinal close-up, point A.

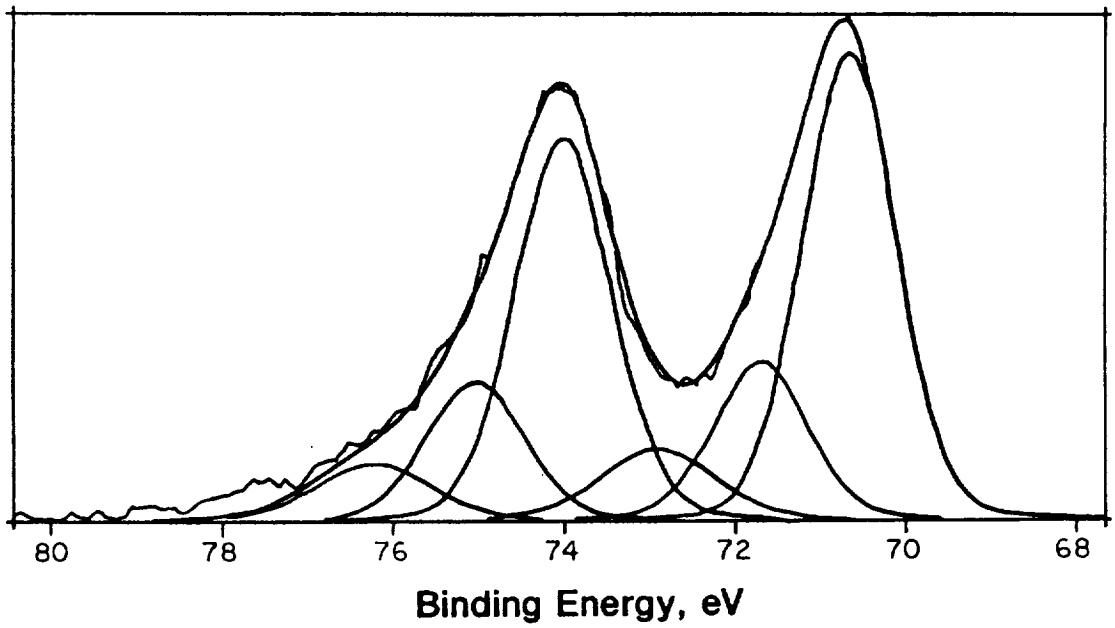

Figure 10. Platinum 4f ESCA spectrum of the Hughes $Pt/Ce/TiO_2$ catalyst.

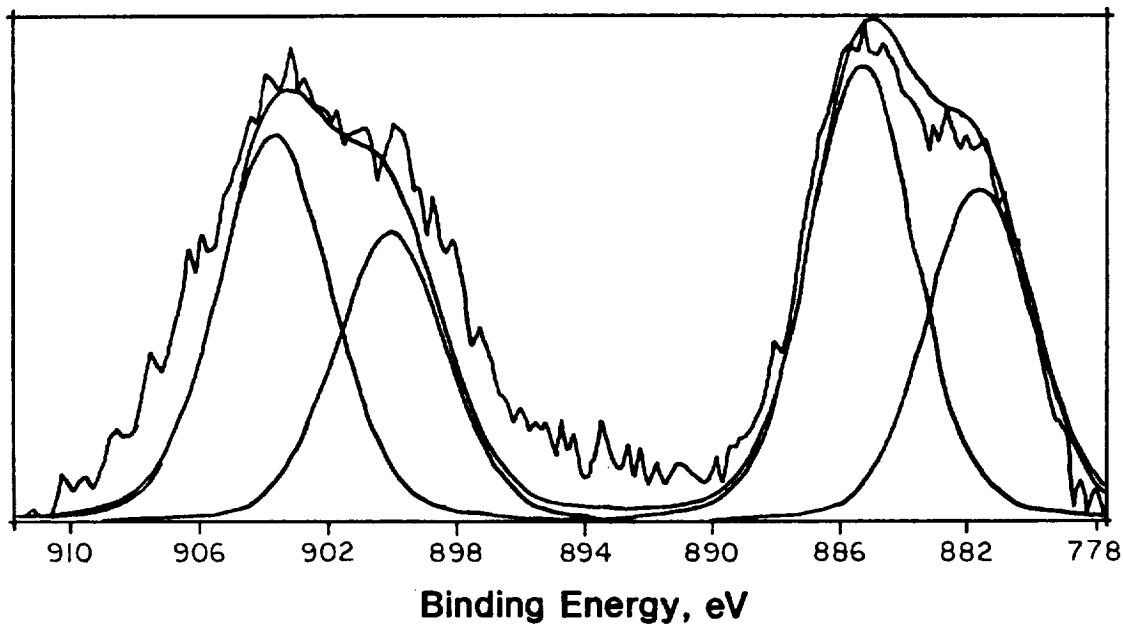

Figure 11. Cerium 3d ESCA spectrum of the Hughes $Pt/Ce/TiO_2$ catalyst.

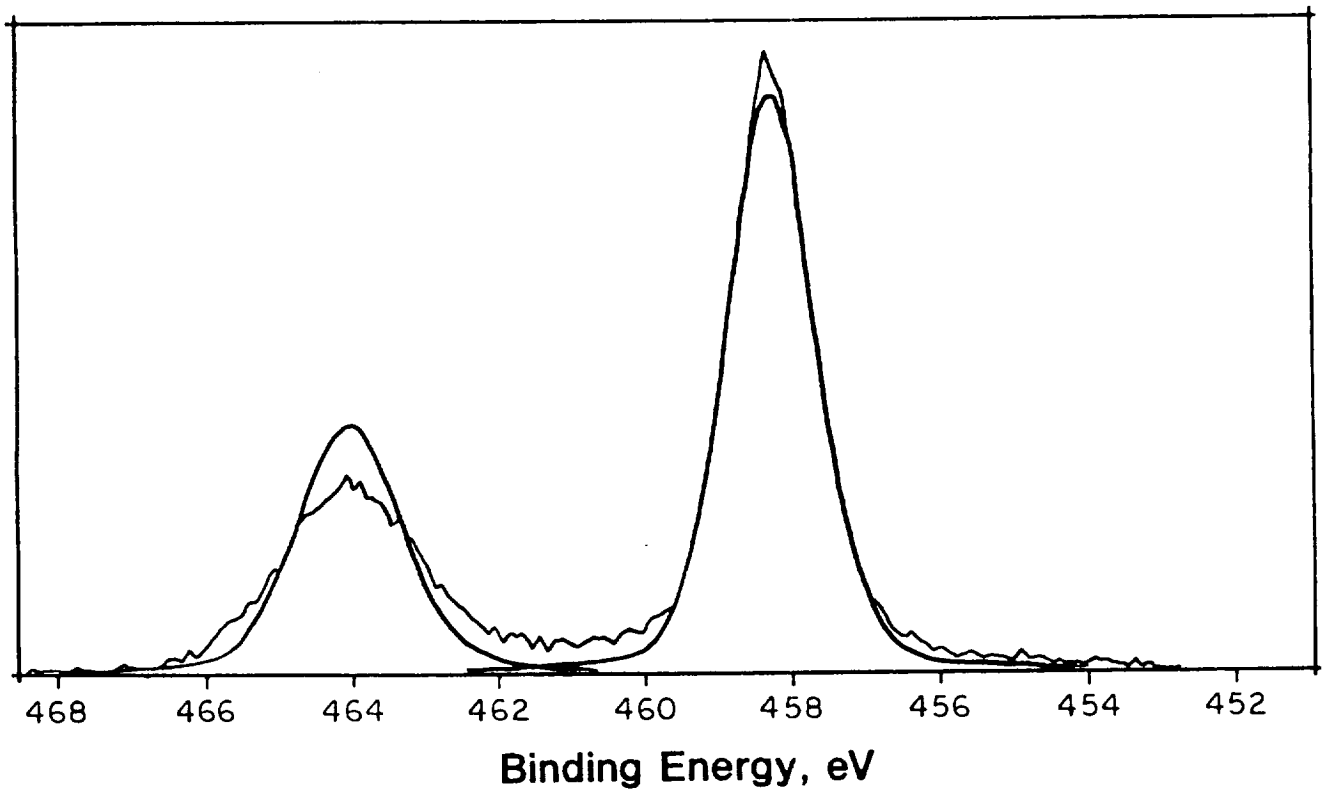

Figure 12. Titanium 2p ESCA spectrum of the Hughes $Pt/Ce/TiO_2$ catalyst.